VOL. 1, NO. 4, OCTOBER 1987 J. THERMOPHYSICS 327

Steady-State Ablation of an Arrhenius Material by External Heating

W. Börsch-Supan* and L. W. Hunter†
Johns Hopkins University, Laurel, Maryland

This paper calculates the recession speed and surface temperature of materials that thermally decompose over a range of temperatures according to a first-order Arrhenius rate law. Due to in-depth reactions, the surface is mushy and the surface temperature is not only unknown in advance, but also requires a careful definition. An application to Teflon includes improved calculations of the in-depth distribution of density and temperature. The results strongly depend on the heat exchange processes in the evolving gas and adjacent boundary layer.

Nomenclature

A = Arrhenius pre-exponential factor
$c(T)$ = specific heat of polymer
$c_g(T)$ = specific heat of gas
$c_\Lambda^{(0)}(\sigma)$ = see Eq. (22)
$c_\Lambda^{(1)}(\sigma)$ = see Eq. (22)
F_+ = total heat flux at cutoff density
F_s = external heat flux at surface (Landau case)
I_∞ = incoming radiation flux
$i(T)$ = specific enthalpy of polymer
$i_g(T)$ = specific enthalpy of gas
$k(T)$ = Arrhenius reaction rate for gasification
$\ell(T)$ = latent heat (consumed by gasification of 1 mass unit of polymer)
P = porosity fraction, $= 1 - \sigma$
r = recession speed
T = temperature (equal for both gas and polymer at a given x)
T^* = Arrhenius activation temperature
T_- = inside temperature of solid
T_+ = temperature at cutoff density
T_Δ = temperature of free gas stream
T_s = surface temperature (Landau case)
V_g = velocity of gas with respect to solid polymer
x = space coordinate (moving)
x_+ = value of x at cutoff density
γ = heat exchange coefficients in boundary condition
ϵ = emissivity
Λ = $\lambda/\bar{\lambda}$
Λ_g = $\lambda_g/\bar{\lambda}$, λ_g conductivity of gas, see Eq. (29)
λ = conductivity, may depend on ρ and ρ_g
$\bar{\lambda}$ = conductivity of compact solid ($P = 1$)
ρ = "apparent" density of solid polymer, $= \bar{\rho} \cdot (1 - P)$
ρ_g = "apparent" density of gas, $= \bar{\rho}_g \cdot P$
$\bar{\rho}, \bar{\rho}_g$ = "true" densities, without and within pores, respectively
σ = relative apparent density, $= \rho/\bar{\rho}$
σ_+ = cutoff density
σ_B = Stefan-Boltzmann constant
τ = $\ell n\, \sigma^{-1}$
$\phi_E(z^{-1})$ = see Eq. (20)
$\Phi_{\Lambda,T}(\sigma)$ = see Eq. (18)
$\phi_1(T, \sigma)$ = see Eq. (13)
$\phi_2(T_+, \sigma)$ = see Eq. (22)

I. Introduction

MANY materials ablate over a range of temperatures according to an Arrhenius rate law. Examples are polymers[1] undergoing thermal decomposition and carbon[2] during combustion. It is desirable to understand how these "Arrhenius materials" respond to a heat flux when the surface temperature is unknown. Indeed, the existence of the surface is questionable, since mass loss can occur at both interior and surface temperature, implying a "mushy" zone.

The thermal degradation of Teflon was investigated by Lengellé.[3] In steady state, the equations of his model for first-order reactions give a solution in which the mushy zone extends indefinitely to the outside. Hence, he introduced a kind of surface or cutoff density as a parameter and came up with a relation between the recession speed and the temperature at this density.

As already pointed out by Kindelan and Williams,[4] this relation needs to be supplemented by a second relation describing an overall energy balance—a relation taking into account the heat exchange with the outside. Reference 4 neglects in-depth mass flux but did find in-depth heat consumption with an Arrhenius temperature-dependence.

We shall take up Lengellé's model for first-order reactions and imbed his relation into a system that includes external heat exchange, thereby showing how the recession speed and surface temperature can be determined simultaneously from other data. We also discuss the in-depth behavior of density and temperature, employing a more elementary mathematical approach than Lengellé and thereby improving on his approximations.

Compared to our earlier paper,[5] the case treated here differs in the following respects:

1) The heat absorption from radiation now is assumed to take place in a very thin layer near the surface (e.g., due to a high absorption coefficient), where the absorption can be incorporated into a boundary condition.

2) We include the heat transfer from the outside through conductive processes in a gaseous boundary layer adjacent to the solid surface.

3) We include the evaporated gas in the system and assume it to be in thermal contact with the remaining solid, thus considering a "mushy material."

4) As a rough model, we use the linear dependence of total conductivity on the density in the mushy zone, with one free parameter (pure-gas conductivity).

Received Aug. 18, 1986; revision received March 2, 1987.

*Professor of Mathematics. (On leave from Johannes Gutenberg-Universität, Mainz, FRG).

†Chemist, Applied Physics Laboratory. Member AIAA.

The different behavior of the temperature distribution in the outer part of the mushy zone in the present paper as compared to Ref. 5 is mainly due to the factors 1 and 2.

II. Basic Equations

We describe the one-dimensional problem with a space coordinate x, which is considered to be moving to the left with a steady-state recession speed r. The basic equations are as follows.

Mass conservation for the solid polymer yields

$$r\frac{\mathrm{d}\rho}{\mathrm{d}x} = -k(T)\rho \tag{1}$$

where $r\,\mathrm{d}/\mathrm{d}x$ is the time derivative in the steady-state case and $k(T)$ the Arrhenius' ablation rate given below. Mass conservation for the gas evolved from the polymer yields

$$r\frac{\mathrm{d}\rho_g}{\mathrm{d}x} + \frac{\mathrm{d}}{\mathrm{d}x}(\rho_g V_g) = k(T)\rho \tag{2}$$

Note that ρ and ρ_g denote "apparent" densities, i.e., masses of solid and gas contained in the same unit volume that may be considered to contain some mixture of gas-filled pores and solid. Hence, $1-\rho/\bar{\rho} = 1-\sigma$ also denotes the porosity fraction P.

Energy conservation leads to

$$\begin{aligned}&\left[c(T)\rho r + c_g(T)\rho_g(r+V_g)\right]\frac{\mathrm{d}T}{\mathrm{d}x} + \frac{\mathrm{d}}{\mathrm{d}x}\left(-\lambda\frac{\mathrm{d}T}{\mathrm{d}x}\right)\\ &\quad = -k(T)\rho\ell(T)\end{aligned} \tag{3}$$

Here, it is assumed that both the solid and the evolving gas have the same temperature at a given x. The second term describes the divergence of conductive heat flow, where the mixed conductivity λ resulting from conduction in both the solid and gas may depend on ρ and T. On the right-hand side, we have the heat consumed by gasification. Mass flux by gas diffusion has been neglected, since it is assumed to be small compared to the bulk flow of gas.

Between the latent heat, specific enthalpies, and specific heats, the following relations hold:

$$\ell(T) = i_g(T) - i(T) \tag{4a}$$

$$i(T) = i(T^{(0)}) + \int_{T^{(0)}}^{T} c(T')\,\mathrm{d}T' \tag{4b}$$

$$i_g(T) = i_g(T^{(0)}) + \int_{T^{(0)}}^{T} c_g(T')\,\mathrm{d}T' \tag{4c}$$

where $T^{(0)}$ is some reference temperature.

The Arrhenius reaction rate is

$$\begin{aligned}k(T) &= A\exp\left(-\frac{T^*}{T}\right) = k(T^{(0)})\exp\left[\frac{T^*}{T^{(0)}}\cdot\left(1-\frac{T^{(0)}}{T}\right)\right]\\ &= k(T^{(0)})\exp\left[-\frac{T^*}{T^{(0)}}\cdot\left(1-\frac{T}{T^{(0)}}\right)\right]\\ &\quad\times\exp\left[-\frac{T^*}{T^{(0)}}\cdot\frac{(T^{(0)}-T)^2}{T^{(0)}T}\right]\end{aligned} \tag{5}$$

where $T^{(0)}$ is again some reference temperature, not necessarily the same as in Eq. (4).

Since the reaction rate is never zero for positive temperatures, the degradation rate is never zero even at great depths. This means that an exact steady-state recession is not possible. Even so, for room temperatures, the reaction rate is extremely slow and we can put it to zero below a certain temperature without changing the system too much. Then, a steady state is possible when the left end temperature is below room temperature (see Ref. 5).

The boundary conditions inside the solid are

$$\lim_{x\to-\infty}\rho(x) = \bar{\rho} \tag{6}$$

$$\lim_{x\to-\infty}\rho_g(x) = 0 \qquad \lim_{x\to-\infty}(\rho_g V_g)(x) = 0 \tag{7a,b}$$

$$\lim_{x\to-\infty}T(x) = T_- \qquad \lim_{x\to-\infty}\left(\lambda\frac{\mathrm{d}T}{\mathrm{d}x}\right)(x) = 0 \tag{8a,b}$$

Note that for sufficiently smooth functions, Eq. (8b) follows from Eq. (8a) and should not be counted as an independent boundary condition.

In order to obtain a "closed" system of equations, we have to introduce a right-side boundary to the physical system and the corresponding boundary conditions. Before doing so, we first simplify the system by eliminating the variables ρ_g and V_g by integrating the sum of Eqs. (1) and (2) from $-\infty$ to some arbitrary x using the boundary conditions of Eqs. (6) and (7). This yields

$$\rho_g(r+V_g) = (\bar{\rho}-\rho)r = r\bar{\rho}(1-\sigma) \tag{9}$$

This equation describes *global mass conservation* from $-\infty$ to x. Using it in Eq. (3), we obtain

$$\begin{aligned}\frac{\mathrm{d}}{\mathrm{d}x}\left(\lambda\frac{\mathrm{d}T}{\mathrm{d}x}\right) &= r\left[c\bar{\rho} + (c_g-c)(\bar{\rho}-\rho)\right]\frac{\mathrm{d}T}{\mathrm{d}x} + \ell(T)k(T)\rho\\ &= r\bar{\rho}c(T)\frac{\mathrm{d}T}{\mathrm{d}x} + r\frac{\mathrm{d}}{\mathrm{d}x}\left[\ell(T)(\bar{\rho}-\rho)\right]\\ &= r\bar{\rho}\frac{\mathrm{d}}{\mathrm{d}x}\left[i(T) + \ell(T)(1-\sigma)\right]\end{aligned} \tag{10}$$

The system we are left with consists of the two differential equations (1) and (10) of first and second order, respectively, and the boundary conditions, Eqs. (6) and (8), at the left end. The unknowns are the functions ρ and T, and the parameter r. We still have to specify two further conditions at the right end. Besides, the position of the origin must be fixed in order to obtain uniqueness.

Specifying these conditions poses some problems, since our system does not have a natural right boundary with a sharp surface: Eq. (1) shows that the solid density will decrease and may do so very quickly as x increases, provided that the temperature is high, but it never reaches zero. This suggests taking $x=\infty$ as the right boundary. However, this would introduce difficulties into the proper formulation of the heat transfer from the outside, since from the heat balance equation it would follow that the temperature goes to infinity as $x\to\infty$. Therefore, we close the system at some finite x, which, in principle, could be either 1) the edge of the gas boundary layer at the free gas stream, which means that we include the gas boundary layer with its internal heat exchange into our system, or 2) some artificially chosen point in the surfacial zone of the solid where the boundary conditions can be stated with a reasonable degree of approximation. The results may then depend on the choice of the boundary point (or actually the boundary density), as was the case in Lengellé's investigation.

For case 1, radiation and reradiation must be incorporated into the equations of internal heat transfer by including supplementary terms in Eq. (10). For case 2, we may consider the radiation and reradiation that concentrated in the boundary.

Since the heat exchange processes in the gas boundary layer may be complicated and not even sufficiently known, we concentrate its global effects into a Newton-type boundary condition and deal with case 2 only.

The boundary conditions at the right end $x = x_+$ ($= 0$, say) are then

$$\sigma(x_+) = \sigma_+ \tag{11}$$

with the chosen cutoff density σ_+, and

$$\lambda \frac{dT}{dx}\bigg|_{x=x_+} = F_+ = F_c + I_\infty - \epsilon\sigma_B T_+^4 \tag{12}$$

with F_+ being the total heat flux from outside, composed of the conductional heat flux F_c in the boundary layer, the given radiation I_∞, and the Boltzmann reradiation term, computed with the temperature T_+ at the cutoff density. The conductional heat flux F_c may be either given or connected to the difference between the "surface" temperature T_+ and the temperature T_Δ of the free gas stream, e.g., by Newton's law.

Since all of the terms in Eq. (10) are written as derivatives, we may proceed by integrating this equation from $-\infty$ to some arbitrary x, thereby incorporating the left-hand boundary condition given by Eq. (8). Thus, we obtain

$$\lambda \frac{dT}{dx} = r\bar{\rho}[i(T) - i(T_-) + \ell(T)(1-\sigma)] \equiv r\bar{\rho}\phi_1(T,\sigma) \tag{13}$$

where we have introduced the abbreviation ϕ_1 (T,σ). This equation states a *global energy balance* for the interval from $-\infty$ to x, the left-hand side being the energy introduced by conduction from the right, whereas the right-hand side describes the consumption of that heat by warming the solid (including the part of the sensible heat taken away by the evolving gas) and by gasification. From another point of view, the right-hand side is the energy content convected from the slab "$-\infty$ to x" to the outside by the movement of the solid and the flow of the evolving gas in unit time.

III. Comparison to Landau's Relation

Landau[6] has given a formula for the recession speed of a melting semi-infinite medium, where melting occurs at a fixed temperature (the melting temperature) and at the surface of the medium only. His equation is

$$r = \frac{F_s}{\bar{\rho}[i(T_s) - i(T_-) + \ell(T_s)]} \tag{14}$$

where the subscript s means "at the surface" and F_s is the external heat flux into the medium at the surface. This equation states that the external heat introduced to the medium is used to warm the solid (enthalpy difference) and melt it. Furthermore, since the melting temperature T_s is given, the equation allows for an explicit determination of the recession speed from the external heat flux F_s.

In our model, the degradation process is different, since it takes place in depth according to Eq. (1) and therefore at different temperatures (since the transport of heat into the interior requires a nonzero temperature gradient). Also, no kind of "melting temperature" is specified by the Arrhenius law.

The heat balance relation described by Eq. (13) holds at every point $x \le x_+$, but the equation may be evaluated at $x = x_+$ with the numerator replaced by the heat flow from outside according to Eq. (12) in order to obtain a relation quite comparable to Landau's relation. For a reasonably good approximation of the recession speed, we may even replace σ_+ by zero. Thus, we obtain

$$r = \frac{F_+}{\bar{\rho}[i(T_+) - i(T_-) + \ell(T_+)(1-\sigma_+)]} \tag{15}$$

It should be noted, however, that, in contrast to Landau's problem, the temperature T_+ at the density σ_+ is not known in advance. It turns out that it can be determined from differential equations (1) and (13) with the boundary conditions of Eqs. (6) and (8a), although it depends in turn on the recession speed r. Therefore, an *implicit* system of *two* equations for the *two* unknowns r and T_+ must be solved assuming the external flow F_+ is given.

IV. Temperature Density Relation

The required supplementary relation between T_+, σ_+, and r was given by Lengellé[3] in approximate form. It can be interpreted as providing the "surface" temperature that is required by the Arrhenius law to ablate the surface at the rate given by Landau's relation. We derive Lengellé's relation in a different, more elementary way, thereby improving some of his approximations and allowing for nonconstant conductivity λ. In order to avoid obscuring the role of T_+, we do not introduce nondimensional variables.

Since the differential equations (1) for ρ (or σ) and (13) for T do not contain x explicitly, thus reflecting the translation invariance of the problem, one can eliminate x completely. Dividing Eq. (1) by Eq. (13) we obtain a differential equation for σ as a function of T or vice versa,

$$\frac{d\sigma}{dT} = -\frac{1}{r^2}\frac{\bar{\lambda}}{\bar{\rho}}\frac{k(T)\Lambda(\sigma;T)\sigma}{\phi_1(T,\sigma)} \tag{16}$$

with the boundary condition

$$\sigma = 1 \quad \text{at} \quad T = T_- \tag{17}$$

This differential equation can be solved approximately by separation of variables using the fact that the strongest dependence on T is observed in $k(T)$. Considering, for the time being, the dependence of T on σ in Λ and ϕ_1 to be given, we obtain

$$\Phi_{\Lambda,T}(\sigma) = \int_\sigma^1 \frac{\phi_1[T(\sigma'),\sigma']}{\Lambda[\sigma';T(\sigma')]\sigma'}\,d\sigma' = \frac{1}{r^2}\frac{\bar{\lambda}}{\bar{\rho}}\int_{T_-}^{T} k(T')\,dT'$$

$$\approx \frac{1}{r^2}\frac{\bar{\lambda}}{\bar{\rho}}\int_0^T k(T')\,dT' \tag{18}$$

where the boundary condition of Eq. (17) has been used and the integral on the right-hand side has been extended to the lower limit zero (which is a very small change and in agreement with the fact that a change on this order of magnitude is necessary to achieve steady state). Observe that $\Phi_{\Lambda,T}(\sigma)$ depends on the functions $\sigma' \to \Lambda(\sigma')$ and $\sigma' \to T(\sigma')$ and not just on the values of $\Lambda(\sigma)$ and $T(\sigma)$ for the specific σ under consideration.

The right-hand side integral of Eq. (18) then can be evaluated exactly in terms of the "exponential integral" (e.g., see Abramowitz and Stegun[7]) and need not be approximated by the exponential function as Lengellé did by neglecting the last factor in the last member of Eq. (5). Hence, we shall have the deviations by this approximation under control,

$$\int_0^T k(T')\,dT' = A\int_0^T \exp\left\{-\frac{T^*}{T'}\right\}dT' = AT^*\int_{T^*/T}^{\infty} e^{-\xi}\frac{d\xi}{\xi^2}$$

$$= AT^*\frac{E_2(T^*/T)}{T^*/T} \tag{19}$$

where the transformation $T^*/T' = \xi$ has been used. For large values of the argument, $Z = T^*/T$, according to Kindelan and Williams,[4] we have the representations

$$\frac{E_2(Z)}{Z} \equiv \frac{e^{-Z}}{Z^2}\Phi_E(Z^{-1})$$

$$\sim \frac{e^{-Z}}{Z^2}\left(1 - \frac{2!}{Z} + \frac{3!}{Z^2} - \frac{4!}{Z^3} + - \cdots\right)$$

$$\approx \frac{e^{-Z}}{Z^2}\cdot\left[\frac{c_1 + c_2 Z^{-1}}{1 + b_1 Z^{-1} + b_2 Z^{-2}} + Z\bar{\epsilon}(Z)\right] \tag{20}$$

with $b_1 = 5.03637$, $b_2 = 4.19160$, $c_1 = 0.99997$, $c_2 = 3.03962$, $|\bar{\epsilon}(Z)| < 10^{-7}$ for $10 \leq Z < \infty$, and the inequalities

$$\frac{e^{-Z}}{Z(Z+2)} < \frac{E_2(Z)}{Z} \leq \frac{e^{-Z}}{Z(Z+1)} \qquad \text{for } Z > 0 \tag{21}$$

The approximation obtained by Lengellé with matching expansions can also be achieved by simply replacing $T(\sigma')$ by the constant T_+ in the left-hand integral of Eq. (18),

$$\int_\sigma^1 \frac{\phi_1(T(\sigma'),\sigma')}{\Lambda(\sigma';T(\sigma'))\sigma'}\,\mathrm{d}\sigma' \approx \int_\sigma^1 \frac{\sigma_1(T_+,\sigma')}{\Lambda(\sigma';T_+)\sigma'}\,\mathrm{d}\sigma' \equiv \phi_2(T_+,\sigma)$$

$$= \phi_1(T_+,0)\int_\sigma^1 \frac{\mathrm{d}\sigma'}{\Lambda(\sigma';T_+)\sigma'} - \ell(T_+)\int_\sigma^1 \frac{\mathrm{d}\sigma'}{\Lambda(\sigma';T_+)}$$

$$\equiv \phi_1(T_+,0)\,c_\Lambda^{(1)}(\sigma) - \ell(T_+)\,c_\Lambda^{(0)}(\sigma) \tag{22}$$

This may be justified by observing that the integrand tends to be largest for the smallest values of σ'; hence, the values σ' near σ_+ give the most important contribution to the integral if σ is confined to the neighborhood of the surface.

By using Eqs. (19) and (20) in the right-hand side of Eq. (18), we obtain

$$A\,\exp\left(-\frac{T^*}{T}\right) = \frac{T^*}{T^2}\cdot\frac{r^{2}_{\bar{p}}\quad \Phi\Lambda, T(\sigma)}{\lambda\quad \Phi_E(T/T^*)}$$

where the strongest dependence on T has been cast to the left-hand side.

The recession speed may be eliminated from this equation by using Eq. (15). Then we obtain

$$A\exp\left(-\frac{T^*}{T}\right) = \frac{T^*}{T^2}\frac{F_+^2}{\bar{\lambda}\bar{\rho}}\frac{\Phi_{\Lambda,T}(\sigma)}{[\phi_1(T_+,\sigma_+)]^2\Phi_E(T/T^*)} \tag{23}$$

In this equation, besides the cutoff density σ_+ as a parameter of the problem, the corresponding "surface" temperature T_+ appears. We determine it by specifying Eq. (23) at the "surface,"

$$A\exp\left(-\frac{T^*}{T_+}\right) = \frac{T^*}{T_+^2}\frac{F_+^2}{\bar{\lambda}\bar{\rho}}\cdot\frac{\Phi_{\Lambda,T}(\sigma_+)}{[\phi_1(T_+,\sigma_+)]^2\Phi_E(T_+/T^*)} \tag{24}$$

From Eqs. (23) and (24) the function $\sigma \rightarrow T(\sigma)$ and the "surface" temperature T_+ may be obtained by simultaneous iteration.

A first approximation for T_+, separated from the determination of $T(\sigma)$, will be achieved when in $\phi_{\Lambda,T}$ the temperature function is replaced by the constant T_+, which replaces $\Phi_{\Lambda,T}(\sigma_+)$ by $\phi_2(T_+,\sigma_+)$. Equation (24) then yields

$$A\exp\left(-\frac{T^*}{T_+}\right) = \frac{T^*}{T_+^2}\frac{F_+^2}{\bar{\lambda}\bar{\rho}}\frac{\phi_2(T_+,\sigma_+)}{[\phi_1(T_+,\sigma_+)]^2\Phi_E(T_+/T^*)} \tag{25}$$

Equation (25) is a generalization of Eq. (All) in Ref. 4. Equation (25) reduces to Eq. (All) in Ref. 4 when Φ_E is replaced by 1, σ_+ is replaced by 0 in ϕ_1, and ϕ_2 is appropriately simplified. In the defining Eqs. (18) and (22) for ϕ_2, Λ is replaced by 1, σ' is set equal to 1 in the denominator, and $\sigma = \sigma_+$ is replaced by 0.

Equation (25) must still be treated iteratively, e.g., by employing successive substitution to its fixed point form

$$T_+ \approx T^*\Big/\left[\ell n\frac{\bar{\lambda}A}{\bar{\rho}T^*} - 2\,\ell n r + 2\,\ell n T_+ + \ell n\Phi_E\left(\frac{T_+}{T^*}\right) - \ell n\phi_2(T_+,\sigma_+)\right] \tag{26}$$

where Eq. (15) is to be used for r. After T_+ has been determined that way, we obtain the function $\sigma \rightarrow T(\sigma)$ approximately from Eq. (23), with $\Phi_{\Lambda,T}(\sigma)$ replaced by $\phi_2(T_+,\sigma)$, or from its fixed-point form

$$T \approx T^*\Big/\left[\ell n\frac{\bar{\lambda}A}{\bar{\rho}T^*} - 2\,\ell n r + 2\,\ell n T + \ell n\Phi_E\left(\frac{T}{T^*}\right) - \ell n\phi_2(T_+,\sigma)\right] \tag{27}$$

Implicitly, this "temperature-density relation," with Φ_E replaced by 1 and $\Lambda \equiv 1$, was already contained in Lengellé's paper, but he did not discuss it further; he restricted himself to the corresponding specialized case of Eq. (26) and discussed the relation between T_+ and r for some adopted "surface" densities σ_+.

Going to the limit $\sigma_+ \rightarrow 0$ does not give reasonable results since one can show that, at least in the case of given flux F_+, the solution T_+ of Eq. (25) would go to $+\infty$. Because of Eq. (1), $\sigma_+ \rightarrow 0$ implies $x_+ \rightarrow \infty$. Hence, physically, this limit does not make sense, since it amounts to introducing the heat energy at a far outside point from which it would have to travel a long way by conduction to reach the zone where the main ablation occurs.

On the other hand, for reasonable values of σ_+ (say 10^{-1}–10^{-3}), the change of T_+ with changing σ_+ is quite moderate, since the dominant σ_+-dependent term to be subtracted in the denominator of Eq. (26) is $\ell n\sigma_+^{-1}$ (if we assume constant Λ in this range), which changes from 0.834 to 1.933. In turn, this results in a change in T_+ of about 2.8%, i.e., for $T_+ \approx 1000$°K in a change by 28°K if we assume a ratio T^*/T_+ of about 40. (For the data on Teflon given by Lengellé, the corresponding change induced in the recession speed would be −1.5%, approximately.) Observe, however, that the change in temperature by 28°K will change $k(T)$ by a factor near three.

An improvement of the approximation for T_+ and $T(\sigma)$ as obtained from Eqs. (25–27) may be achieved if the expression $\Phi_2(T_+,\sigma)$ is replaced by a better approximation to $\Phi_{\Lambda,T}(\sigma)$. This, in turn, may be obtained by evaluating the left-hand integral in Eq. (18) or (22) with $T(\sigma')$ taken from the approximation resulting from Eq. (27). In fact, this procedure may be repeated iteratively in order to achieve an exact expression for $\Phi_{\Lambda,T}(\sigma)$ in case of convergence. The evaluation of the integral in Eq. (18) must be done numerically, e.g., by a weighted trapezoidal rule,

$$\Phi_{\Lambda,T}(\sigma_j) = \int_{\sigma_j}^1 \frac{\phi_1[T(\sigma'),\sigma']}{\Lambda(\sigma')\sigma'}\,\mathrm{d}\sigma'$$

$$= \int_{\sigma'=\sigma_j}^{\sigma'=1}\phi_1[T(\sigma'),\sigma'][-\mathrm{d}c_\Lambda^{(1)}(\sigma')]$$

$$\approx \sum_{i=j}^{n-1}\frac{\phi_1[T(\sigma_{i+1}),\sigma_{i+1}] + \phi_1[T(\sigma_i),\sigma_i]}{2}$$

$$\cdot[c_\Lambda^{(1)}(\sigma_i) - c_\Lambda^{(1)}(\sigma_{i+1})] \qquad j = 1,2,\ldots n-1, \tag{28}$$

where a suitable partition of the interval (0,1): $0 < \sigma_1 < \sigma_2 < \cdots < \sigma_{n-1} < \sigma_n \leq 1$ has been used and the dependence of Λ on T has been dropped. As to the contribution of the last subinterval, one should be cautious in taking $\sigma_n = 1$, since $T(\sigma)$ drops down to its value $T(1) = T_-$ only very close to $\sigma = 1$, such that a trapezoidal approximation to the integrand is not advisable. Instead, one may replace $\phi_1[T(1),1]$ by some value extrapolated linearly with respect to σ from values in the last interval.

A different approach would be to integrate the differential equation (16) with initial condition [Eq. (17)] by a numerical method. Observe that, because of the enormous changes of $k(T)$ during the course of the integration, the step size should be adapted to these changes. Since the differential equation contains the parameter r, which in turn via Eq. (15) depends on its solution (namely, the value $T = T_+$ resulting in $\sigma = \sigma_+$), one has to proceed iteratively. As an initial approximation, one may choose T_+ from the solutions of Eqs. (26) and (15).

V. Dependence on Conductivity in the Gas

The integral in Eq. (22) and, therefore, the temperature-density relations for Eqs. (23–27) strongly depend on the function $\Lambda(\sigma)$ (even with neglected temperature dependence of the latter), i.e., on assumptions on the conductivity in the evolving gas (or on any other heat exchange processes involved) and on the pore structure, which together lead to an effective conductivity $\bar{\lambda} \cdot \Lambda(\sigma)$ in the gas/polymer mixture in the ablation zone.

Since gas conductivity in general is two or three orders of magnitude smaller than solid conductivity, $\Lambda(\sigma) = \sigma$ might be a good approximation, although some theoretical models of conductivity suggest an even steeper decrease of $\Lambda(\sigma)$ with decreasing σ, i.e., increasing porosity (e.g., see Brailsford and Mayor[8]). On the other hand, if other conduction-like processes are involved, then as more pores open toward the gas boundary layer, this decrease could be weakened or even inverted into a rise of $\Lambda(\sigma)$ with decreasing σ. Therefore, we shall introduce the (still very simple) model with linear dependence on σ,

$$\Lambda(\sigma) = \Lambda_g(1 - \sigma) + \sigma \tag{29}$$

as a base for discussion with $\Lambda_g = \Lambda(0)$ as a parameter. Equation (29) includes the case of constant $\Lambda \equiv 1 (\Lambda_g = 1)$ assumed by Lengellé. The two integrals on the right-hand side of Eq. (22) can then be evaluated to give

$$c_\Lambda^{(1)}(\sigma) = \int_\sigma^1 \frac{d\sigma'}{\Lambda(\sigma')\sigma'} = \frac{1}{\Lambda_g}\ell n\sigma^{-1} + \frac{1}{\Lambda_g}\ell n\left[\Lambda_g(1-\sigma)+\sigma\right] \tag{30}$$

provided $\Lambda_g \neq 0$ and

$$c_\Lambda^{(0)}(\sigma) = \int_\sigma^1 \frac{d\sigma'}{\Lambda(\sigma')} = \frac{1}{\Lambda_g - 1}\ell n\left[\Lambda_g(1-\sigma)+\sigma\right] \tag{31}$$

provided $\Lambda_g \neq 1$. For the special cases not covered by these formulas, by limiting considerations, we obtain

$$\begin{aligned} c_\Lambda^{(1)}(\sigma) &= \sigma^{-1} - 1 && \text{if } \Lambda_g = 0 \\ &= \ell n\sigma^{-1} && \text{if } \Lambda_g = 1 \end{aligned} \tag{32}$$

$$\begin{aligned} c_\Lambda^{(0)}(\sigma) &= \ell n\sigma^{-1} && \text{if } \Lambda_g = 0 \\ &= 1 - \sigma && \text{if } \Lambda_g = 1 \end{aligned} \tag{33}$$

In any of these cases, as $\sigma \to 0$, the term with $c_\Lambda^{(1)}(\sigma)$ will be dominant and will go to infinity in logarithmic fashion (except in the case $\Lambda_g = 0$, where a hyperbolic law applies). The limit could be made finite only when $\Lambda(\sigma) \to \infty$ as $\sigma \to 0$, e.g., $\Lambda(\sigma) = \sigma^{-\delta}$ with some $\delta > 0$.

VI. Spatial Distribution of Density and Temperature

In deriving the temperature-density relation, the space variable has been eliminated from the differential equations. However, if one wants to know about the spatial distribution of density and temperature across the ablation zone, one has to reintroduce x by using Eq. (1), which can be written as

$$-\frac{\sigma\, dx}{d\sigma} = \frac{dx}{d\tau} = \frac{r}{k[T(\sigma)]} \tag{34}$$

where $\tau = \ell n\, \sigma^{-1}$ is introduced as a new density variable and $T(\sigma)$ is to be introduced from the temperature-density relation given implicitly in Eqs. (18), (22), (23), and (27). Using Eq. (18) together with Eqs. (19) and (20) leads to

$$\begin{aligned} \frac{r}{k[T(\sigma)]} &= \frac{\bar{\lambda}}{r\bar{\rho}} \cdot \frac{[T(\sigma)]^2}{T^*} \frac{\Phi_E[T(\sigma)/T^*]}{\Phi_{\Lambda,T}(\sigma)} \\ &\approx \frac{\bar{\lambda}}{r\bar{\rho}} \cdot \frac{T_+^2 \Phi_E(T_+/T^*)}{T^* \phi_2(T_+, \sigma)} \end{aligned} \tag{35}$$

where, in the rightmost member, the approximation T_+ for $T(\sigma)$ has been used with the σ dependence being left in $\phi_2(\mathrm{T}_+, \sigma)$. Substituting $\sigma = \exp(-\tau)$ and choosing the density

Table 1 Improvement of Lengellé's approximation [Eq. (24)] in the temperature-density relation
$\Lambda_g = 0.1$, $\sigma_+ = 0.01$, $F_+ = 8.0$ cal · cm^{-2} · s^{-1} fixed

Relative density σ	Temperature T, K using Eq. (24)	Improved temperature T, K using Eq. (29)
0.9	908.1	902.4
0.8	925.3	920.4
0.7	937.4	933.2
0.6	947.8	944.2
0.5	957.6	954.5
0.4	967.4	964.8
0.3	978.1	976.0
0.2	990.7	989.1
0.1	1008.1	1007.0
0.05	1021.6	1020.8
0.02	1035.4	1034.8
0.01	1043.4	1043.0

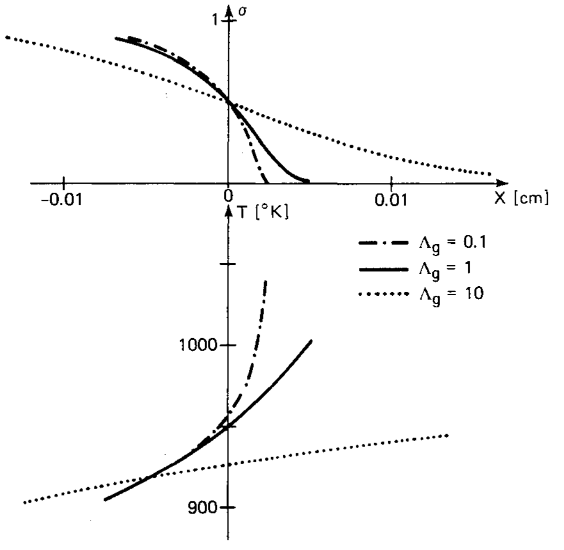

Fig. 1 Temperature and density distributions, $F_+ = 8.0$ cal · cm^{-2} · s^{-1}.

Table 2 Recession speeds and temperatures for different conductivities and cutoff densities $F_+ = 8.0$ cal • cm^{-2} • s^{-1}

Λ_g	Cutoff density σ_+	Temperatures T, K at $\sigma = 0.1$	0.5	0.9	Boundary temperature T_+, K	Recession speed r, 10^{-3} cm · s^{-1}
0.1	0.1	1010.8	959.7	909.7	1010.8	6.25
	0.01	1008.1	957.6	908.1	1043.4	5.84
	0.001	1007.7	957.4	908.1	1060.8	5.76
1	0.1	985.2	952.3	908.4	985.2	6.34
	0.01	982.7	950.0	906.5	1001.6	5.96
	0.001	982.3	949.9	906.5	1012.0	5.90
10	0.1	946.7	928.4	901.1	946.7	6.47
	0.01	944.3	926.2	899.1	956.5	6.09
	0.001	944.1	926.0	899.0	964.0	6.03

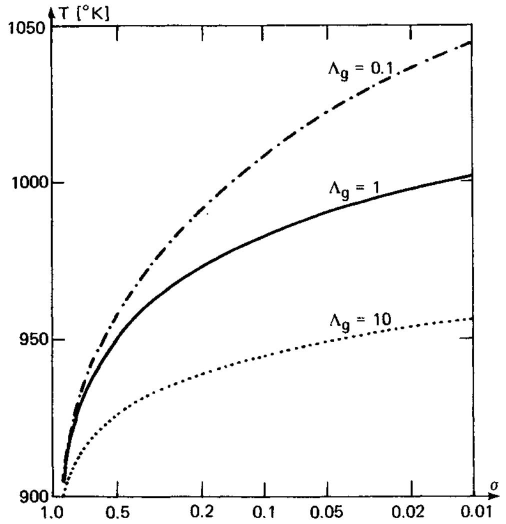

Fig. 2 Temperature-density relation, $F_+ = 8.0$ cal • cm^{-2} • s^{-1}.

$\sigma_0 = \exp(-\tau_0)$ as origin for x, we obtain the first approximation

$$x \approx \frac{\bar{\lambda} T_+^2 \Phi_E(T_+/T^*)}{r\bar{\rho}T^*} \cdot \int_{\tau_0}^{\tau} \frac{\mathrm{d}\tau'}{\phi_2(T_+, e^{-\tau'})} \tag{36}$$

But even if we know the explicit dependence of ϕ_2 on σ such as the cases dealt with in Sec. V, the integral seems not to be treatable by explicitly known functions. Hence, a numerical integration by a trapezoidal rule is used to obtain the relation between x and σ in the ablation zone. After computing the temperature-density relation, a better approximation to x may be obtained by using the factor $[T(\sigma')]^2$ within the integral instead of T_+^2 in front of it,

$$x = \frac{\bar{\lambda}\Phi_E(T_+/T^*)}{\gamma\bar{\rho}T^*} \int_{\tau_0}^{\tau} \frac{[T(e^{-\tau'})]^2}{\phi_2(T_+, e^{-\tau'})}\,\mathrm{d}\tau' \tag{37}$$

Outside of the ablation zone, it is more advisable to use the relation between the temperature and space variables in Eq. (13) for the in-depth relation. Replacing σ by 1 we have

$$\frac{\mathrm{d}T}{\mathrm{d}x} = r\frac{\bar{\rho}}{\bar{\lambda}}[i(T) - i(T_-)] \tag{38}$$

which reduces to a linear differential equation if the specific heat c of the polymer is temperature independent,

$$\frac{\mathrm{d}T}{\mathrm{d}x} = r\frac{\bar{\rho}}{\bar{\lambda}}c(T - T_-) \tag{39}$$

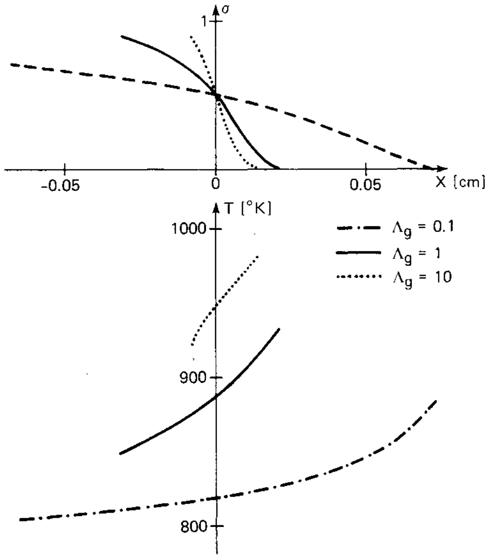

Fig. 3 Temperature and density distributions, $F_+ = \gamma(T_\Delta - T_+)$, $\gamma = \Lambda_g\bar{\lambda}/\Delta$.

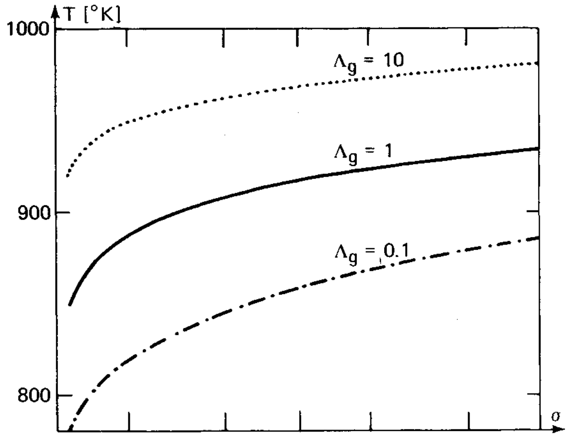

Fig. 4 Temperature-density relation, $F_+ = p(T_\Delta - T_+)$, $\gamma = \Lambda_g\bar{\lambda}/\Delta$.

Its solution is well known,

$$T(x) = T_- + (T(x_1) - T_-)\cdot\exp\left[\frac{r\bar{\rho}c}{\bar{\lambda}}(x - x_1)\right] \tag{40}$$

where $T(x_1)$ is to be chosen to match the temperature in the ablation zone at $x = x_1$.

Table 3 Recession speeds, temperatures, and external heat fluxes for different conductivities and cutoff densities $F_+ = \gamma(T_\Delta - T_+), \gamma = \Lambda_g \bar{\lambda}/\Delta = 6.34 \times 10^{-3} \Lambda_g$ cal · cm^{-2} · s^{-1} · K^{-1}, $\Delta = 0.1$ cm, $T_\Delta = 1200$ K

Λ_g	Cutoff density σ_+	Temperatures T, K at			Boundary temp. T_+, K	Recession speed r, 10^{-3} cm · s^{-1}	External heat flux F_+, cal · cm^{-2} · s^{-1}
		$\sigma = 0.1$	0.5	0.9			
0.1	0.1	862.7	823.8	785.0	862.7	0.18	0.21
	0.01	858.2	819.8	781.6	884.2	0.16	0.20
	0.001	856.6	818.5	780.6	895.5	0.15	0.19
1	0.1	921.0	891.5	852.2	921.0	1.4	1.8
	0.01	916.8	887.7	848.8	933.5	1.3	1.7
	0.001	915.3	886.4	847.7	941.4	1.2	1.6
10	0.1	972.3	953.2	924.7	972.3	11.5	14.4
	0.01	968.2	949.3	921.1	980.8	10.4	13.9
	0.001	966.6	947.8	919.8	987.3	10.1	13.5

VII. Numerical Results

The results obtained so far have been applied to the ablation of Teflon, using the same data as in Lengellé's paper[3] and three types of boundary conditions [Eq. (12)]. In all cases, we used the approximation $\phi_2(T_+, \sigma)$ for $\Phi_{\Lambda,T}(\sigma)$, since it turned out that the difference in the results was unimportant (see Table 1 for the worst of the cases computed here). Observe that this difference is particularly small at cutoff density.

Figures 1 and 2 compare the results for different conductivity-density relations, characterized by $\Lambda_g = 0.1, 1$, and 10, for a fixed cutoff density $\sigma_+ = 0.01$ and a flux of $F_+ = 8.0$ cal · cm^{-2} · s^{-1}. Observe in Table 2 that the recession speeds do not change much since they are determined essentially by the flux: $r = 5.84 \times 10^{-3}$, 5.96×10^{-3}, and $6.09 \times 10^{-}3$ cm/s for $\Lambda_g = 0.1$, 1, and 10, respectively. As compared to the constant conductivity case $\Lambda_g = 1$, lowering the conductivity in the surface zone ($\Lambda_g = 0.1$) causes a larger temperature gradient, particularly where the density is low. This leads to higher temperatures near the surface and a faster ablation rate, i.e., a thinner outside part of the ablation zone. On the other hand, for $\Lambda_g = 10$, the conductivity will be changed in the opposite direction, but to a much larger extent, in both the outer and inner parts of the ablation zone. Hence, we see a much smaller temperature gradient; the ablation is distributed over a much thicker zone and the temperatures are lower. Figure 2 shows T vs σ. Here, the influence of Λ_g is much simpler, underlining the importance of the temperature-density relation.

As compared to the influence of conductivity, the influence of the cutoff density σ_+ is much lower, as is seen from Table 2, although a limit is not approached as $\sigma_+ \to 0$. Introducing the flux at a higher density ($\sigma = 0.1$) and closing the system there reduces the total amount of heat needed to warm and gasify the solid, which explains the higher recession speed. On the other hand, closing the system at very low densities leads to high boundary temperatures, although the temperature-density relation is changed only slightly. This is due to the high temperature gradient with respect to σ, particularly with low conductivity.

The picture changes considerably if the heat is introduced from the outside by conduction through a gas boundary layer whose conductivity is obtained by extension from the law used in the mushy zone. This amounts to a coefficient $\gamma = \lambda_g/\Delta = \Lambda_g \bar{\lambda}/\Delta$ in Newton's cooling law $F_+ = \gamma(T_\Delta - T_+)$ where T_Δ is the temperature at the edge of the boundary layer and Δ the thickness of that layer, both kept fixed at $T_\Delta = 1200$ °K and $\Delta = 0.1$ cm in our computations, and $\bar{\lambda} = 6.34 \times 10^{-4}$ cal · cm^{-1} · s^{-1} · K^{-1}. In this case, low conductivity leads to low heat flux and small recession speed and, hence, to low temperatures and a very broad ablation zone, whereas high conductivity has the opposite influence (see Figs. 3 and 4).

The influence of the cutoff density as seen in Table 3 is still small, although higher than in the constant flux case. This can be explained by the fact that at a higher cutoff density the temperature T_+ will be lower and, hence, the heat flux introduced will be higher, which amounts to a further increase of recession speed beyond the effect described in the constant-flux case.

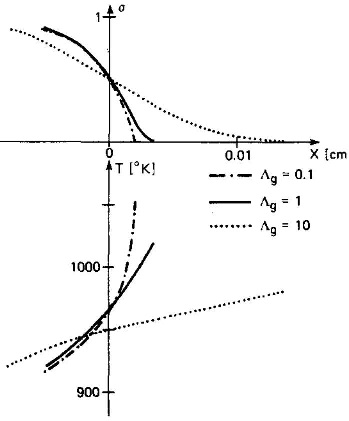

Fig. 5 Temperatures and density distributions, $F^+ = \gamma(T_\Delta - T_+)$, $\gamma = 0.0634$ cal · cm^{-2} · s^{-1} · K^{-1}.

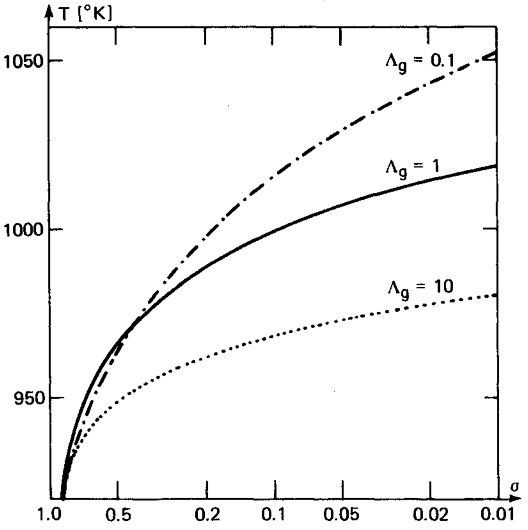

Fig. 6 Temperature-density relation, $F^+ = \gamma(T_\Delta - T_+)$, $\gamma = 0.0634$ cal · cm^{-2} · s^{-1} · K^{-1}.

Table 4 Recession speeds, temperatures, and external heat fluxes for different conductivities and fixed cutoff density
$\sigma_+ = 0.01$, $F_+ = \gamma(T_\Delta - T_+)$,
$\gamma = 6.34 \times 10^{-2}$ cal · cm^{-2} · s^{-1} · K^{-1} fixed, $T_\Delta = 1200$ K

	Temperatures T, K at			Boundary temperature	Recession speed	External heat flux
Λ_g	$\sigma = 0.1$	0.5	0.9	T_+, K	r, 10^{-3} cm · s^{-1}	F_+, cal · cm^{-2} · s^{-1}
0.1	1015.8	964.7	914.6	1051.7	6.84	9.41
1	999.4	965.8	921.1	1018.8	8.48	11.5
10	968.2	949.3	921.1	980.8	10.45	13.9

In a third combination, we use a flux coupled to the temperature difference between the boundary-layer edge and the cutoff density point by a (rather large) proportionality constant of $\gamma = 0.0634$ cal · cm^{-2} · s^{-1} · K^{-1} corresponding to a large conduction-like heat exchange in the boundary layer. However, in the mushy zone, we employ different conductivities, thus describing a situation in which the heat exchange in the mushy zone is more or less hindered by the pore structure.

The results, as seen in Figs. 5 and 6 and Table 4, are quite similar to those for constant flux, but we observe higher fluxes and recession speeds, as well as higher temperatures and somewhat thinner ablation zones.

In all of the computations, for the sake of simplicity, the approximation given by Eq. (36) for x has been used, although, due to temperature deviations from T_+, Eq. (37) may lead to up to 20% thinner ablation zones.

It should be mentioned that, in cases with strong dependence of the heat flux on the surface temperature as in cases with high gas conductivity, the iterative solution of Eq. (26) with r inserted from Eq. (15) and F_+ from the corresponding boundary condition, may be slowly or not at all converging. In this case, it is advisable to apply a convergence generating and accelerating procedure such as Steffensen's.[9]

VIII. Conclusions

This paper draws attention to the importance of characterizing the surface of an Arrhenius material, i.e., a material that gasifies at different temperatures with an Arrhenius rate, not only at the surface but also in depth. Experimental experience indicates that the surface can have a quite complicated structure on a microscopic scale. The flow of the evaporating gas may occur through a complicated system of pores and cracks. The heat-transfer mechanisms may include not only conduction, but also some type of flow-related exchange.

In spite of this complicated nature of the system, attempts to treat the problem by a simplified theoretical model are still worthwhile. The approach we have followed in this paper is at first to introduce a cutoff density and to concentrate at this point the heat exchange processes with the outside. The cutoff density also may be looked at as a breakdown density of the mechanical structure of the solid. Furthermore, we have used a simple linear relation between conductivity and density (or porosity) with the pure-gas relative conductivity Λ_g as a parameter. Outside the cutoff location, the conduction-like processes in the gas can be modeled independently by the heat exchange parameter γ in the boundary condition.

In a sense, σ_+ (the cutoff density), Λ_g, and γ characterize the complications at and near the surface. There remains the need for a more detailed model, based on careful experiments, to be realistic. A continuous transition from gas evolving within the solid to the gaseous boundary layer may be part of such a model.

The results presented here show that the influence of the cutoff density, if kept in a certain range, is not very important. The numerical results on the dependence on the conductivity parameters Λ_g and γ, however, reveal that the magnitude and structure of the conductive heat transfer near the surface have a large influence both on the thickness of the mushy zone that develops and on its temperature distribution. It is, therefore, believed that future studies should concentrate on the exact nature and detailed structure of the heat and mass transfer processes.

Acknowledgment

This work was supported by internal research and development funds through a U.S. Navy Contract N00024-85-C-5301. The authors are indebted to S. Favin for assisting with the numerical calculations.

References

[1] Madorsky, S.L., *Thermal Degradation of Organic Polymers*, Krieger Publishing Co., Huntington, NY, 1975.

[2] Tsuiji, H. and Matsui, K., "An Aerothermochemical Analysis of Combustion of Carbon in the Stagnation Flow," *Combustion and Flame*, Vol. 26, 1976, pp. 283–297.

[3] Lengellé, G., "Thermal Degradation Kinetics and Surface Pyrolysis of Vinyl Polymers," *AIAA Journal*, Vol. 8, Nov. 1970, pp. 1989–1996.

[4] Kindelan, M. and Williams, F.A., "Theory for Endothermic Gasification of a Solid by a Constant Energy Flux," *Combustion Science and Technology*, Vol. 10, 1975, pp. 1–19.

[5] Börsch-Supan, W., Hunter, L.W., and Kuttler, J.R., "Endothermic Gasification of a Solid by Thermal Radiation Absorbed in Depth," *International Journal of Heat and Mass Transfer*, Vol. 27, Aug. 1984, pp. 1171–1182.

[6] Landau, H.G., "Heat Conduction in a Melting Solid," *Quarterly of Applied Mathematics*, Vol. 8, 1950, pp. 81–94.

[7] Abramowitz, M. and Stegun, I.A. (eds.) *Handbook of Mathematical Functions*, National Bureau of Standards, Pub. AMS-55, 1964, pp. 228–231.

[8] Brailsford, A.D. and Major, K.G., "The Thermal Conductivity of Aggregates of Several Phases, including Porous Materials," *British Journal of Applied Physics*, Vol. 15, 1964, pp. 313–319.

[9] Stoer, J. and Bulirsch, R., *Introduction to Numerical Analysis*, Springer, New York, Heidelberg, Berlin, 1980, p. 298.